GEOLOGICA CARPATHICA, 52, 5, BRATISLAVA, OCTOBER 2001
277–286

FLUID INCLUSION STUDY ON HYDROTHERMAL As-Au-Sb-Cu-Pb-Zn VEINS IN THE MLYNNÁ DOLINA VALLEY (WESTERN CARPATHIANS, SLOVAKIA)

JURAJ MAJZLAN[1], VRATISLAV HURAI[2] and MARTIN CHOVAN[3]

[1]Department of Geology, University of California at Davis, Davis, California 95616, USA; jmajzlan@ucdavis.edu
[2]Dionýz Štúr Geological Institute, Mlynská dolina 1, 817 04, Bratislava, Slovak Republic
[3]Department of Mineralogy and Petrology, Comenius University, Mlynská dolina G, 842 15 Bratislava, Slovak Republic

(Manuscript received October 31, 2000; accepted in revised form June 13, 2001)

Abstract: A study of fluid inclusions from the ore samples from the Mlynná dolina valley (Nízke Tatry Mts, Western Carpathians) has provided information on the formation conditions of the mineralization. Arsenopyrite and pyrite are accompanied by quartz with CO_2-rich, low-to-moderately saline (3.6–15.4 wt. % NaCl eq.) fluid inclusions with homogenization temperatures of 281–365 °C and estimated trapping pressures between 150 and 350 MPa. Arsenopyrite thermometry suggests a crystallization temperature of 320–380 °C, thus overlapping the fluid inclusion data. Subsequent decrease in temperature and pressure were probably responsible for the fluid devolatilization and the precipitation of stibnite and berthierite at temperatures of 200–250 °C and pressure <100 MPa. Formation conditions of chalcopyrite–tetrahedrite assemblage are poorly constrained due to the paucity of fluid inclusions. These homogenize at 157–187 °C and indicate an aqueous fluid with a salinity of 17.9–22.0 wt. % NaCl eq. Superimposed galena-sphalerite assemblage is hosted by quartz containing fluid inclusions with a salinity of 16.3–22.5 wt. % $CaCl_2$ eq. and homogenization temperatures between 95–202 °C. Preliminary thermometry and mineralogical data for mineralizations of the Mlynná dolina valley suggest a close genetic similarity to other ore deposits in the Nízke Tatry Mts.

Key words: Western Carpathians, Nízke Tatry Mts, ore mineralizations, fluid inclusions.

Introduction

There is a long mining history in the Nízke Tatry Mountains which contain rich ore accumulations (Chovan et al. 1996). In addition to the large ore deposits (cf. Dúbrava, Magurka), numerous smaller deposits were mined in the past. A number of small abandoned mines have been found in the Mlynná dolina valley (Andrusov et al. 1951) but there have been only a few mineralogical studies on these ores (Turan 1961; Stankovič 1976; Majzlan & Chovan 1997).

A detailed fluid inclusion study of the Dúbrava deposit was presented by Chovan et al. (1995) and Chovan et al. (1999). As a continuing effort to understand the conditions of ore deposition in the Nízke Tatry Mts, we have conducted a microthermometric study on the vein quartz associated with mineralization in the Mlynná dolina valley. Our objectives are to determine the fluid inclusion composition, to correlate the timing of inclusion trapping with the growth of ore minerals, and to derive thermodynamic information from equilibrium mineral assemblages in order to understand the conditions under which the mineralization has formed. The ore veins in the Mlynná dolina valley are then compared with other deposits in the Nízke Tatry Mts, and with similar hydrothermal deposits elsewhere, in terms of their mineralogical composition and evolution of hydrothermal fluids.

Geological settings

The Western Carpathians (Fig. 1a) are a collisional Alpidic orogen, which formed after closure of the Tethys Ocean due to the folding and thrusting of the rock complexes. The Western Carpathians can be subdivided into the Outer, Central and Inner Western Carpathians (Plašienka et al. 1997).

The Outer Western Carpathians are represented by the Carpathian Foredeep infilled by Oligocene-Miocene molasse sediments. Only the southernmost part of the Foredeep was incorporated into orogen nappe structure and can be compared with the Subalpine Mollasse Zone in the Eastern Alps. The Central Western Carpathians are further subdivided into the Tatric, Veporic, and Gemeric superunits separated by major mid-Cretaceous thrust-faults. Inner Western Carpathians comprise the Meliatic and Silicic superunits. The oceanic crust of the Meliata Ocean was subducted and metamorphosed into blueschist facies, and later thrust over the Gemeric Superunit. The Silicic Superunit represents the uppermost, mostly non-metamorphosed allochthonous unit.

The Tatric basement of the Central Western Carpathians (Fig. 1b) is composed of large fragments with Variscan nappe structure, composed of Variscan granitoid plutons emplaced within medium- to high-grade metamorphic rocks (Putiš 1992). The Tatric unmetamorphosed sedimentary cover comprises Upper Carboniferous-to-Albian lithological members. Mesozoic sedimentary nappes (Krížna, Choč, and Strážov) were thrust from the south and overlie the Tatric basement/cover complexes. Alpine low-grade metamorphism influenced only the marginal domains of the Central Western Carpathians.

The Nízke Tatry Mountains (Fig. 1b), located in the Central Western Carpathians, are the most extensive mountain range of the Western Carpathians. The Čertovica fault, a major mid-Cretaceous thrust fault, divides the Nízke Tatry Mts into the

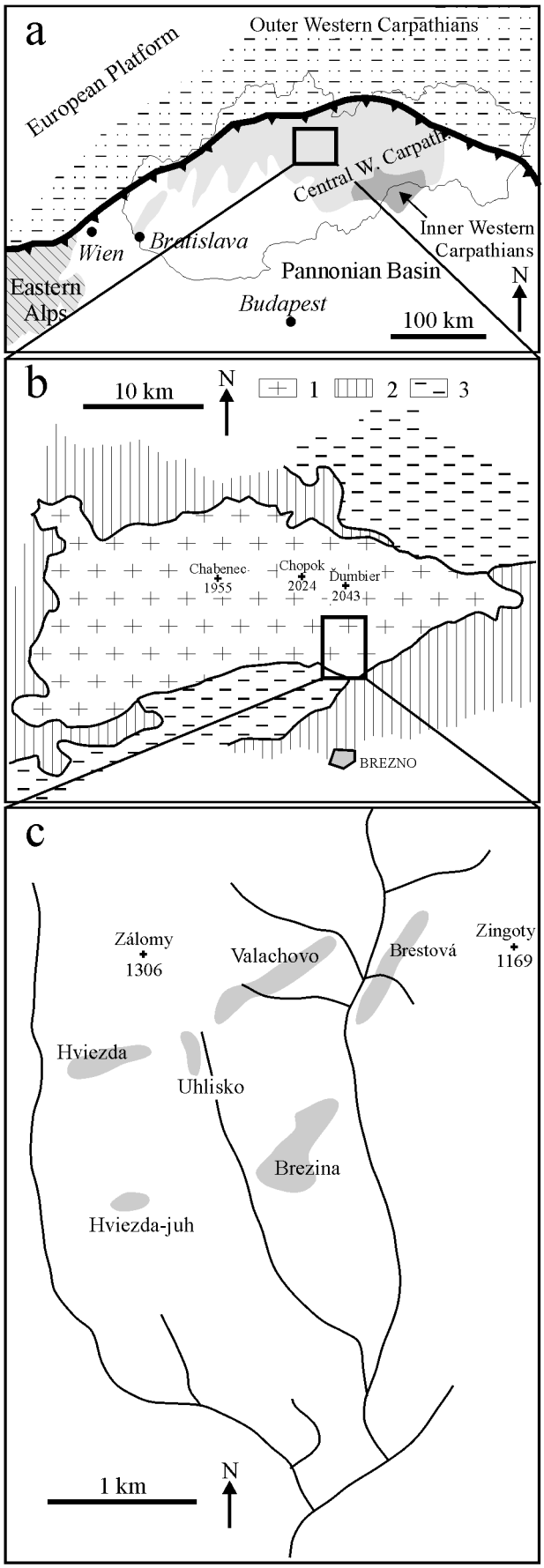

western Tatric part (with Au-Sb deposits Dúbrava, Magurka, Dve Vody, and others), and the eastern Veporic part.

The Paleozoic crystalline complex of the Tatric part of the Nízke Tatry Mts consists of Variscan granites and medium- to high-grade metamorphic rocks, comprising anatectic migmatites, various types of gneisses, and amphibolites (Krist et al. 1988). The crystalline complex and its autochthonous Mesozoic sedimentary cover were overthrusted by the Mesozoic (Krížna and Choč) nappes.

The most important sulphide mineralizations in the Nízke Tatry Mts are hosted by the Tatric crystalline complex. The formation of these mineralizations is believed to be linked with Variscan metamorphism and the final stages of the granitoid plutons emplacement (Putiš 1992) in an overthickened continental crust of the Variscan orogen. The veins, stringers, and disseminated ores of Au-Sb±(As, Pb, Cu, W) are localized inside regional mylonite zones of N-S and E-W direction, accompanied by brittle fault structures penetrating the crystalline complex. A weak Alpine reactivation induced fault formation within the crystalline complex and the overlying Permian-Mesozoic sequences. It is generally accepted that despite being insufficient for a large-scale metal remobilization, the low-grade Alpine metamorphism generated smaller siderite-sulphide veins.

The ore occurrences in the Tatric crystalline complex of the Nízke Tatry Mts were classified by Chovan et al. (1996) who distinguished the uranium, molybdenum, tungsten (scheelite), As-Fe-Au (arsenopyrite-pyrite with gold), Au-quartz, antimony with Fe, Cu, Pb, Sb, Bi, Ag sulphides, Pb (galena) — base-metals, siderite with Cu sulphides, and hematite mineralizations.

The Mlynná dolina is a north-south-oriented valley in the Nízke Tatry Mts (Fig. 1c), north of the town of Brezno (Fig. 1b). The dominant rock types are migmatites with small amphibolite and lamprophyre bodies belonging to the Tatric crystalline complex (Biely & Bezák 1997). The northern part of the Mlynná dolina valley is developed in the Carboniferous granitoid rocks of the Králička and Ďumbier types (Biely & Bezák 1997). The Čertovica lineament crops out several kilometers east of the valley, thus defining the contact between the high-grade metamorphic rocks and granitoids of the Tatric complex, and the weakly metamorphosed rocks of the Veporic complex (Fig. 1b). In the southern part of the Mlynná dolina

Fig. 1. a) A sketch of Central Europe showing the Outer, Central, and Inner Western Carpathians. The thin solid line is the state border of the Slovak Republic. The area delimited by the heavy outlined box is expanded in 1b; **b)** a schematic geological map of the Nízke Tatry Mountains (after Slavkay & Chovan 1996). 1 — Tatric (Cretaceous–Permian and crystalline core), 2 — Veporic (crystalline core) and Krížna Nappe (Cretaceous–Permian), 3 — Choč Nappe (Cretaceous–Upper Carboniferous). Elevation points indicated by crosses, elevation given in meters above sea level. The area delimited by the heavy outlined box is expanded in 1c; **c)** location of the abandoned mine fields and waste dumps in the area of the Mlynná dolina valley. Elevation points indicated by crosses, elevation given in meters above sea level. Solid lines represent streams.

valley, the crystalline complex dips beneath the sub-autochthonous and allochthonous Mesozoic sedimentary sequences.

Methods

Shallow pits and abandoned mine dumps were sampled at Valachovo, Hviezda, Brestová, Uhlisko, Hviezda-juh, and Brezina occurrences in the Mlynná dolina valley (Fig. 1c). Mineral associations in these localities have been studied by Majzlan & Chovan (1997) in polished and thin sections in reflected and transmitted light. Fluid inclusions described in this work were studied in 0.2–0.3 mm thick doubly polished wafers. After petrographic documentation at room temperature, phase transitions in the inclusions have been measured using a LINKAM THMSG-600 freezing-heating stage. The instrument was calibrated using synthetic $K_2Cr_2O_7$ (398 °C) and with natural inclusions of known composition at the triple point of pure CO_2 (–56.6 °C), and at the melting point of bi-distilled water (0 °C). The calibration at the triple point of CO_2 was performed daily when measurements at sub-ambient temperatures were carried out. The precision of the measurements between –50 and +100 °C is ±0.2 °C. The precision of the measurements T > 100 °C for homogenization to the liquid phase is about ±2 °C. Salinities of the fluids were calculated from the equations of Oakes et al. (1990), Darling (1991), Diamond (1992), and Bodnar (1993) for the appropriate systems. The isochores for the fluid inclusions were calculated using the FLINCOR software (Brown 1989) for the H_2O–NaCl and H_2O–NaCl–CO_2 systems, and by the algorithm of Zhang & Frantz (1987) for the H_2O–$CaCl_2$ system.

Results

Mineralogy

Ore veins in the Mlynná dolina valley comprise several distinct mineral assemblages (Majzlan & Chovan 1997). Their tentative crystallization sequence is depicted in Fig. 2. A more reliable temporal relationship is unclear due to poor exposure and the inaccessibility of the underground workings. Consequently, the strike, slope, and thickness of the veins is not exactly known. The only direct evidence for a cross-cutting relationship is the occurrence of tetrahedrite veinlets in fractured arsenopyrite and pyrite crystals, as observed on a microscopic scale in reflected light. Additional indirect evidence comes from the degree of deformation in the gangue minerals (Table 1),

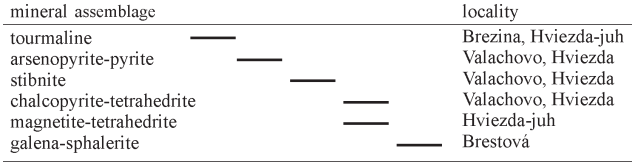

Fig. 2. A tentative paragenetic sequence of the mineral assemblages distinguished in the Mlynná dolina valley. The localities of the mineral assemblages after Majzlan & Chovan (1997).

Table 1: Mineral assemblages of the ore veins in Mlynná dolina valley (after Majzlan & Chovan 1997) and the deformation features of their minerals. Electron microprobe analyses of the sulphides and identification schemes for some rarer sulphosalts were taken from Majzlan & Chovan (1997).

Assemblage	Major minerals	Minor minerals	Deformation features
tourmaline	tourmaline, quartz	pyrite	quartz strongly deformed into ribbons; tourmaline crystals fragmented and bent
arsenopyrite -pyrite	arsenopyrite, pyrite, quartz	gold, rutile, K-feldspar	quartz with undulatory extinction; arsenopyrite and pyrite crystals fractured
stibnite	stibnite, pyrite, quartz	berthierite, zinckenite, gold, Fe-dolomite	quartz and stibnite with undulatory extinction; stibnite shows pressure-induced twinning
chalcopyrite -tetrahedrite	chalcopyrite, tetrahedrite, quartz	chalcostibite, Bi-jamesonite, Bi-berthierite, kobellite, krupkaite	quartz with undulatory extinction; sulphides not affected by deformation
magnetite-tetrahedrite	magnetite, hematite, tetrahedrite, chalcopyrite, siderite, quartz		quartz with undulatory extinction; Fe-oxides and sulphides not affected by deformation
galena-sphalerite	galena, sphalerite, quartz	pyrite, chalcopyrite	none

formation *PT* conditions estimated in this work, and a comparison with other ore bodies in the Nízke Tatry Mts. The mineral assemblages are listed in Table 1.

Arsenopyrite and pyrite of the *arsenopyrite-pyrite assemblage* form large (1–2 mm) euhedral crystals uniformly dispersed in quartz and feldspar. Minute gold grains (average size 20 μm, maximum size 90 μm) are enclosed by arsenopyrite or are found in cracks within the arsenopyrite. The temporal relationship between quartz and the sulphides could not be discerned from the available samples.

The sulphides of the *stibnite assemblage* form aggregates and veinlets that appear to post-date quartz. Textural relationships show that berthierite postdates stibnite. In some cases, the emplacement veinlets and acicular crystals of berthierite have been accompanied by the recrystallization of quartz and resulted in a 'halo' of quartz surrounding the berthierite.

The *chalcopyrite-tetrahedrite assemblage* was emplaced in pre-existing vein structures that contained arsenopyrite and pyrite.

Magnetite and hematite of the *magnetite-tetrahedrite assemblage* form octahedral and tabular crystals, respectively. Pseudomorphs of magnetite after hematite and vice versa can be commonly observed in polished sections. Both oxides appear to be younger than abundant siderite. Tetrahedrite and chalcopyrite form veinlets in the weathered iron oxyhydroxide matrix. The samples were collected from shallow pits and advanced weathering to a mixture of earthy iron oxyhydroxides,

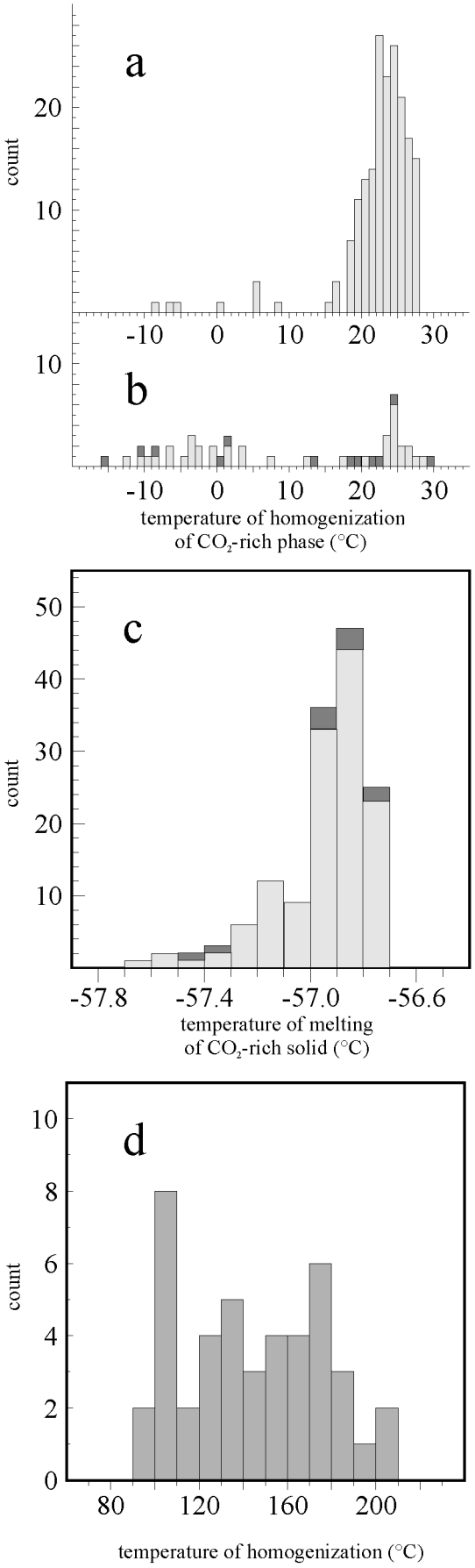

covelline, and malachite precluded more precise determination of the mineral succession.

The sulphides of the *galena-sphalerite assemblage* post-date quartz.

Typology of fluid inclusions and microthermometry data

The number of observable phases in fluid inclusions at room temperature was the basis for distinguishing several inclusion types, which are listed in Table 2. Most inclusions are monophase (liquid-only), less commonly two (liquid + gas) phases have been observed. The size of the inclusions ranges from <5 μm up to 20 μm. The samples of chalcopyrite-tetrahedrite and magnetite-tetrahedrite assemblages contain few primary fluid inclusions, and no inclusions were found in the samples of the tourmaline assemblage. Therefore, in the remaining text, most emphasis is laid on the arsenopyrite-pyrite, stibnite, and galena-sphalerite assemblages. No measurements were performed on the secondary inclusions, whose trails are ubiquitous in quartz accompanying all mineral assemblages.

Microthermometric measurements were interpreted in terms of available experimental data (Oakes et al. 1990; Darling 1991; Diamond 1992; Bodnar 1993). The phase transitions measured were the melting temperature of carbon dioxide ($T\mathrm{mCO_2}$), eutectic temperature (Te), melting temperature of the gas clathrate ($T\mathrm{m_{clat}}$), and ice ($T\mathrm{m_{ice}}$), the partial homogenization temperature of the CO_2-rich phase ($T\mathrm{hCO_2}$) and total homogenization temperature (Th). All phase transitions were estimated at a heating rate of 0.1 °C/min. The $T\mathrm{m_{clat}}$ values were obtained using the sequential freezing method (Collins 1979). The results of the microthermometric measurements are listed in Table 3.

Arsenopyrite-pyrite assemblage

Quartz that hosts arsenopyrite, pyrite and gold contains abundant carbonic-aqueous, and sparse carbonic fluid inclusions. Small (<1 μm) inclusions are the most abundant, causing 'cloudiness' of the quartz. Larger inclusions that survived tectonic deformation occur either randomly in areas with abundant small inclusions or in small clusters in clearer quartz. The inclusions bear no clear signs of a secondary origin according to conventional criteria (Roedder 1984), however, they cannot be unambiguously assigned a primary origin.

The $T\mathrm{hCO_2}$ values divided the inclusions with the carbonic phase into two groups (Fig. 3a,b): the inclusions with relatively low $T\mathrm{hCO_2}$ (–15 to +12 °C) (hereafter referred to as carbonic-aqueous I) and inclusions with higher $T\mathrm{hCO_2}$ (+15 to +28 °C) (hereafter carbonic-aqueous II). In the quartz with arsenopyrite and pyrite, the former group of inclusions is more

Fig. 3. a,b) Histogram of $T\mathrm{hCO_2}$ values of the carbonic-aqueous I and II (light gray bars) and carbonic inclusions (dark gray bars): a — from quartz associated with stibnite and berthierite, b — from quartz associated with arsenopyrite and pyrite. **c)** Histogram of $T\mathrm{mCO_2}$ values for the carbonic-aqueous I and II (light gray bars) and carbonic inclusions (dark gray bars). **d)** Histogram of Th values for the aqueous inclusions from quartz associated with galena and sphalerite.

Table 2: Types of fluid inclusions from the Mlynná dolina valley.

phases discernible at room temperature	type
liquid, gas, or supercritical CO_2	carbonic
liquid, gas, or supercritical CO_2 with aqueous phase	carbonic-aqueous
liquid, gas, or supercritical CO_2 with aqueous phase and halite crystal	carbonic-aqueous-halite
aqueous phase and vapour	aqueous
aqueous phase and vapour, crystals of solid phases	aqueous-solid

abundant than the latter. No *T*h values have been obtained for the carbonic-aqueous I inclusions due to their decrepitation prior to total homogenization. The *T*mCO_2 values in all CO_2-bearing inclusions have been close to the triple point of pure CO_2 (Fig. 3c, Table 3), indicating only minor amounts of other gaseous components besides CO_2.

Stibnite assemblage

Quartz associated with stibnite, berthierite and gold contains numerous carbonic-aqueous and aqueous inclusions, and rare carbonic-aqueous-halite inclusions. The carbonic-aqueous inclusions I are rarely found in the quartz associated with stibnite. The carbonic-aqueous inclusions II (Fig. 4) occur either isolated or in small clusters but their secondary or primary origin is equivocal. A total of 17 *T*h measurements (Fig. 5, Table 3) were made for the carbonic-aqueous II inclusions that homogenized to either liquid or gas. Most carbonic-aqueous II inclusions decrepitated between 250 and 300 °C due to high internal overpressure. Therefore, each successful *T*h measurement was checked by repeated *T*hCO_2 measurement to ensure that the inclusion has not undergone stretching or decrepitation. The carbonic-aqueous-halite fluid inclusions were only found in a small quartz crystal isolated in massive stibnite. Their relationship to other inclusions in the sample is not clear and they were not further characterized.

The aqueous inclusions appear to be pseudosecondary or secondary with respect to the host quartz. In a few cases, the aqueous inclusions were found in healed cracks extending beyond the quartz-penetrating stibnite veinlets. The aqueous inclusions are also found in clear quartz halos around berthierite veinlets or in trails extending from berthierite aggregates and crystals. Occasionally, a jagged interface between the vapor bubble and the liquid phase at temperatures <10 °C suggested the presence of CO_2 hydrate. Many aqueous inclusions decrepitated upon heating. The data for the inclusions for which

Table 3: Chemical and physical properties of the fluids trapped in fluid inclusions in the samples from the Mlynná dolina valley. For the microthermometry measurements, only the minimum and maximum values are reported, with the exception for *T*e where all data are given. Volume estimates have been made at room temperature. (**f.i.** — fluid inclusions.)

f.i. type and mineral assemblage	measured temperatures of phase transitions	size and shape, phase proportions	chemical system, salinity of the aqueous phase, and f.i. density
carbonic f.i. in Q from arsenopyrite-pyrite and chalcopyrite-tetrahedrite assemblages	*T*mCO_2 -57.4 to -56.7 °C, *T*hCO_2 -15.4 to +29.0 °C	≤5 μm, regular shape	system CO_2, density 0.631–1.011 g/cm^3
carbonic-aqueous f.i. I in Q from arsenopyrite-pyrite, stibnite, and chalcopyrite-tetrahedrite assemblages	*T*mCO_2 -57.4 to -56.7 °C, *T*hCO_2 -15.4 to +12.0 °C, *T*m$_{clat}$ 1.5–8.6 °C	≤10 μm, regular shape, occasional necking-down	system H_2O–CO_2–NaCl±KCl, salinity 4.4–14.8 wt.% NaCl eq., density 0.936–1.046 g/cm^3
carbonic-aqueous f.i. II in Q from arsenopyrite-pyrite and stibnite assemblages	*T*mCO_2 -57.6 to -56.7 °C, *T*e -22.5, -22.5, -22.5 °C, *T*hCO_2 15.6 to 28.3 °C, *T*m$_{clat}$ 0.2–8.2 °C, *T*h 281–428 °C	<10 μm, regular, commonly negative crystal shapes, occasional necking-down, CO_2-rich phase ~20–95 vol.%	system H_2O–CO_2–NaCl±KCl, salinity 3.6–15.4 wt.% NaCl eq., density 0.670–1.007 g/cm^3
aqueous f.i. in Q from stibnite assemblage	*T*e -22.5, -22.7 °C, *T*m$_{ice}$ -7.3 to -11.7 °C, *T*h 205–292 °C	usually <10 μm, occasionally up to 20 μm, regular, common negative crystal shapes, low density phase ~20 vol.%	system H_2O–NaCl±KCl, traces of CO_2, salinity 10.9–15.7 wt.% NaCl eq., density 0.904–0.943 g/cm^3
aqueous f.i. in Q from chalcopyrite-tetrahedrite assemblage	*T*m$_{ice}$ -19.5 to -14.1 °C, *T*h 157–187 °C	≤5 μm, regular, occasionally negative crystal shapes, low density phase ~20 vol.%	system H_2O–NaCl, salinity 17.9–22.0 wt.% NaCl eq., density 1.016–1.063 g/cm^3
aqueous f.i. in Q from galena-sphalerite assemblage	*T*e -43, -50 °C, *T*m$_{ice}$ -12.8 to -24.1 °C, *T*h 95–202 °C	<10 μm, usually regular in shape, occasional signs of necking-down, low density phase ~15 vol.%	system H_2O–NaCl–$CaCl_2$, salinity 16.3–22.5 wt.% $CaCl_2$ eq. (density not calculated because NaCl/$CaCl_2$ ratio is not known)

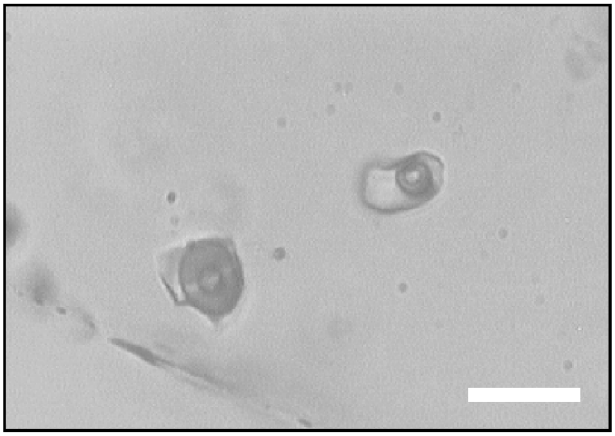

Fig. 4. Two carbonic-aqueous II fluid inclusions in quartz associated with stibnite and berthierite. The inclusions contain different phase proportions, thus indicating a heterogeneous entrapment of two immiscible CO_2-rich and water-rich phases. Microphotograph taken at appr. 20 °C, scale bar represents 10 μm.

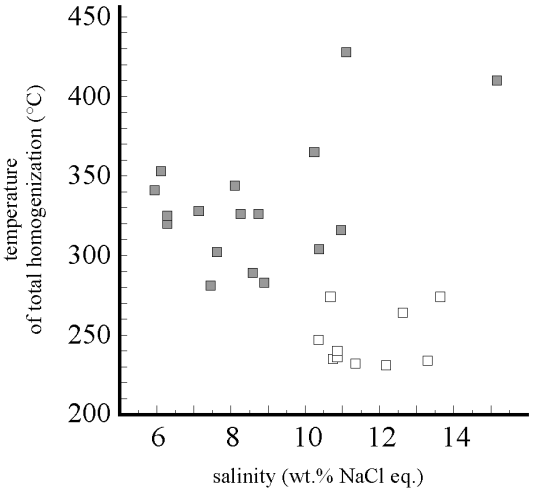

Fig. 5. Plot of salinity and total homogenization temperature of the carbonic-aqueous II (gray squares) and aqueous (open squares) inclusions from quartz associated with stibnite and berthierite.

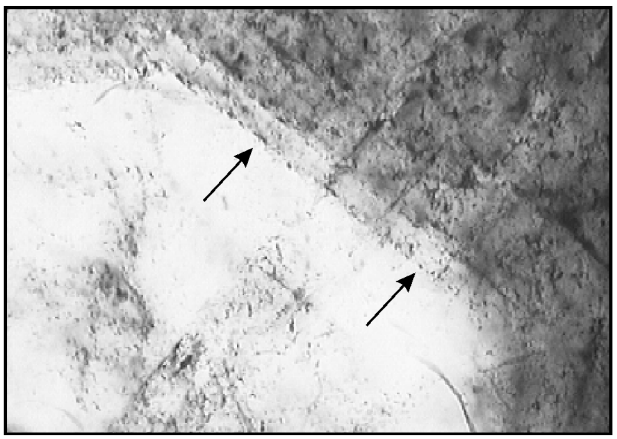

Fig. 6. A subhedral crystal of quartz, hosting galena and sphalerite. Arrows point at fluid inclusions outlining the growth zone of the quartz crystal. The width of the microphotograph corresponds to appr. 1 mm.

both Th and Tm_{ice} values have been measured are plotted in Fig. 5.

Chalcopyrite-tetrahedrite assemblage

Quartz associated with chalcopyrite and tetrahedrite contains carbonic-aqueous and aqueous inclusions. The carbonic-aqueous inclusions are uncommon and found only in a few clusters in clearer quartz. All measured inclusions belong to the carbonic-aqueous I inclusion type (Table 3). Their relationship to the quartz host or the ore minerals is, because of their paucity, unclear. We consider the carbonic-aqueous inclusions in these samples to be related to the early arsenopyrite-pyrite mineralization present in the samples. The aqueous inclusions occur either in cloudy quartz or in clear quartz grains intergrown with copper-bearing minerals, suggesting that they may be related to the copper-bearing ore fluids.

Galena-sphalerite assemblage

Quartz associated with galena and sphalerite contains numerous aqueous inclusions and rare aqueous-solid inclusions. The inclusions occur isolated or as trails that do not intersect grain boundaries or as smaller inclusions delineating the growth zones of the quartz crystals (Fig. 6). The solid phases occur as either transparent cubes, probably halite, or more rarely as unidentified anisotropic acicular crystals. Sphalerite contains sparse, large aqueous fluid inclusions.

Eutectic melting and Tm_{ice} values below eutectic point of the H_2O–NaCl system (Table 3) suggests the presence of chlorides of divalent cations in the fluid (Davis et al. 1990). The aqueous fluid inclusions displayed a range of *T*h values (Table 3) with no sharp maxima (Fig. 3d) and little correlation of salinity with *T*h (Fig. 7). The halite cubes in the aqueous-solid inclusions are too small to reliably measure their dissolution temperature. After cooling to room temperature, the halite crystals did not re-nucleate. Attempts to measure the temperature of incongruent hydrohalite melting indicated metastable hydrohalite transformation at temperatures above 10 °C.

Discussion

The results from fluid inclusion studies combined with petrographic research of ore samples can constrain the *P-T-X* conditions of ore formation. In the samples from the Mlynná dolina valley, however, there are only a few links between the fluid inclusions trapped in quartz and the sulphidic mineralization hosted by the gangue minerals.

Variability of the volumetric ratio between the CO_2- and H_2O-rich phases in the carbonic-aqueous inclusions (Table 3, Fig. 4) accompanying arsenopyrite-pyrite and stibnite indicates a heterogeneous trapping of the CO_2-rich fluid. Therefore, *T*h values of the carbonic-aqueous II inclusions (281–428 °C, Fig. 5) represent the highest possible temperatures of formation. The lowest estimates approach the actual trapping temperatures, while the higher values could correspond either to trapping temperature or to a solvus of a particular random mixture of two coexisting — gas- and liquid-dominated phas-

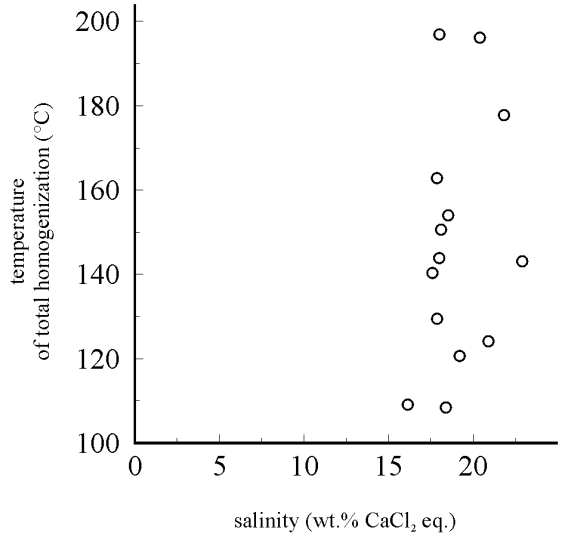

Fig. 7. Plot of salinity and total homogenization temperature for the aqueous inclusions from quartz associated with galena and sphalerite.

es trapped in the individual inclusions. The higher density of the carbonic-aqueous I inclusions in comparison with that of the carbonic-aqueous II inclusions points indirectly to an earlier origin of the former. Therefore, we assume that *T*h values for the carbonic-aqueous I inclusions would be equal or higher than those of the carbonic-aqueous II inclusions. A higher trapping temperature also means a higher trapping pressure. A calculation of the trapping pressure for the carbonic-aqueous inclusions I was precluded by the lack of their *T*h values. The homogenization pressure was calculated for all carbonic-aqueous inclusions II for which the necessary data exist (Fig. 8a), even if the *T*h values have been below the lower applicability limit (350 °C) for the equation of state of Bowers & Helgeson (1983). The carbonic-aqueous inclusions I are interpreted as representing an earlier hydrothermal fluid with temperature and pressure higher than the fluid sampled by the carbonic-aqueous inclusions II. Isochores for the carbonic-aqueous fluid inclusions (Fig. 8a) indicate the lowest approximate formation *PT* conditions at 280 °C and 150 MPa, or higher, possibly reaching ~365 °C and ~350 MPa.

Temperature of arsenopyrite-pyrite deposition may also be constrained using arsenopyrite geothermometry (Kretschmar & Scott 1976). Arsenopyrite crystals contain 30.4 ± 0.2 atomic % As and 0.8 ± 0.2 (2σ) atomic % Co + Ni + Sb (Majzlan & Chovan 1997). Chemical homogeneity of the arsenopyrite and pyrite seen in back-scattered electron images and intergrowth of the two sulphides with no signs of replacement suggests thermodynamic equilibrium between the two phases during crystallization. According to the geothermometer, arsenopyrite should have crystallized at temperatures of 320–380 °C. This estimate allows arsenopyrite composition to deviate from the FeS_2–$FeAs_2$ join and neglects the influence of pressure on the geothermometer (Sharp et al. 1985). The spatial association of arsenopyrite, pyrite and quartz-hosted carbonic-aqueous fluid inclusions, and the overlap between the homogenization temperatures of the inclusions and the arsenopyrite thermometry suggest that the arsenopyrite-pyrite mineralization was derived from the CO_2-rich fluids at a temperature range of 280–380 °C. Similar estimates have been obtained for the same assemblage from the Sb-Au deposit at Dúbrava (Sachan & Chovan 1991; Chovan et al. 1995).

Petrographic observations (occurrence of aqueous inclusions in cracks extending beyond the stibnite veinlets, in halos around berthierite aggregates) suggest that aqueous fluids have precipitated stibnite and berthierite. We suppose that the aqueous fluid was derived from the CO_2-rich fluid by devolatiliza-

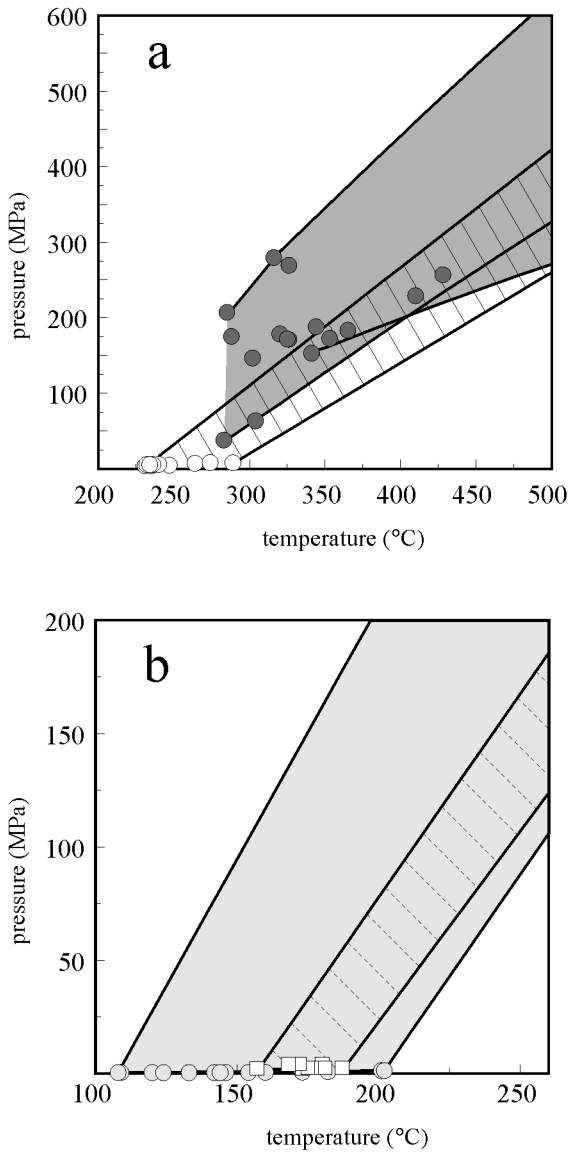

Fig. 8. a) Isochoric envelopes for the inclusions from the arsenopyrite-pyrite (shaded) and stibnite (hatched) assemblages. Homogenization temperatures and pressures are shown for arsenopyrite-pyrite (grey circles) and stibnite (open circles) assemblages. **b)** Isochoric envelopes for the chalcopyrite-tetrahedrite (hatched) and galena-sphalerite (shaded) assemblages, with squares (chalcopyrite-tetrahedrite) and circles (galena-sphalerite assemblage) corresponding to homogenization temperatures and pressures. The isochores for the galena-sphalerite assemblage have been calculated using the volumetric properties of the H_2O–$CaCl_2$ system because the inclusions have been too small to measure temperature of halite dissolution and to derive the $NaCl/CaCl_2$ ratio.

tion and followed the solvus in the H_2O-rich part of the H_2O–CO_2–NaCl system during decompression. Therefore, the estimated homogenization temperatures (205–292 °C) of the aqueous inclusion should be close to the actual trapping temperatures. Isochores of the fluid inclusions (Fig. 8a) suggest trapping pressure of <100 MPa. The estimated temperature range is also consistent with conditions for Sb and S saturation and stibnite precipitation at about ≤250 °C (Williams-Jones & Normand 1997). The predominant Sb and Au species in a near-neutral fluid at temperatures <275 °C are metal thiocomplexes (Seward 1973; Krupp 1988). Loss of sulphur via effervescence causes destabilization of the thiocomplexes and precipitation of sulphides and gold (Krupp 1988). Formation of berthierite post-dating stibnite may correspond to a decrease in sulphur fugacity (Vaughan & Craig 1997) that is induced by effervescence.

The presented data enable a comparison between the mineralizations in the Mlynná dolina valley and elsewhere in the Nízke Tatry Mts, as well as with similar ores in the European Hercynides. Fluid inclusion data from the Dúbrava deposit (Chovan et al. 1995) show the early scheelite and arsenopyrite-pyrite stages precipitated from a CO_2-rich, low salinity (H_2O-NaCl) fluid at 305–355 °C and >200 MPa. We have also found carbonic fluid inclusions in fine-grained pyrite-arsenopyrite ores containing gold from the Dve Vody Sb-Au deposit. Adamia et al. (1989) reported on CO_2 and CH_4 from the Jasenie-Kyslá W-Au deposit indicated by chromatographic analysis of gases liberated during decrepitation of fluid inclusions. In summary, the CO_2-rich, low salinity fluid inclusions commonly occur in the arsenopyrite-pyrite and auriferous mineralizations throughout the Nízke Tatry Mts. They record the *PT* conditions (>300 °C, >100 MPa) of the earliest hydrothermal fluid. Contrasting with this behavior is quartz associated with arsenopyrite, pyrite, and gold from the Vyšná Boca locality, containing only aqueous inclusions with salinities of 2.7–16.3 wt. % NaCl eq. (Smirnov 2000).

Deposition of the early auriferous pyrite-arsenopyrite ores has often been related to low salinity, CO_2-rich fluids containing reduced sulphur species, at a relatively high temperature of 250–400 °C (Lattanzi et al. 1989; Boiron et al. 1990; Ortega et al. 1996). In general, the lode-gold deposits are associated with metamorphic terranes, CO_2-rich fluids, sericitization of the wall-rocks, quartz-dominated veins that are relatively poor in sulphides, and with a high Au : Ag ratio (~10) (Groves et al. 1998). However, the CO_2-rich fluids have not been observed in all Au-As-Sb deposits (Boiron et al. 1989), thus bringing into question the importance of carbon dioxide for transport of these metals.

A common later stage (or stages) following the deposition of the Fe-As sulphides is an assemblage with Sb-Pb-Cu-Zn sulphides, precipitating from lower temperature (150–250 °C) aqueous fluids (e.g. Boiron et al. 1990). Ortega et al. (1996) and Clayton & Spiro (2000) inferred that the aqueous fluids evolved by CO_2-outgassing.

The younger mineralizations in the Nízke Tatry Mts that are rich in Sb, Pb, Zn, and Cu have formed from fluids of higher salinity and lower temperature, with little or no CO_2. Fluid inclusions in quartz with stibnite, sulphosalt, and tetrahedrite indicate a relatively low temperature (105–170 °C), H_2O-NaCl fluid at the Dúbrava deposit (Chovan et al. 1995). Infrared microthermometry data on fluid inclusions in stibnite at Dúbrava indicate primary aqueous fluid inclusion with 3–16 wt. % NaCl eq. and homogenization temperatures mostly between 100–150 °C (Chovan et al. 1999). Preliminary results suggest that the conditions of stibnite precipitation at Dúbrava and Mlynná dolina may be different.

No fluid inclusions related to the magnetite-tetrahedrite mineralization have been found so far. This mineralization is characterized by high oxygen fugacity reflected by presence of di-trivalent (magnetite) and trivalent (hematite) iron oxides. Both chalcopyrite-tetrahedrite and magnetite-tetrahedrite assemblages bear a strong resemblance to the siderite-sulphide ore veins of the Nízke Tatry Mts with respect to their mineralogical composition and textural appearance (cf. Ozdín & Chovan 1999; Ozdín & Pršek 2000).

The latest mineralizations in the Nízke Tatry Mts are related to fluids rich in solutes of divalent metals, most probably $CaCl_2$. The barite stage at Dúbrava originated from H_2O-NaCl-$CaCl_2$ fluids at 105–160 °C (Chovan et al. 1995). Similarly, the lead and zinc ores of the Mlynná dolina valley have formed from a low-temperature, high-salinity NaCl-$CaCl_2$ aqueous fluid. Luptáková et al. (2000) have found $CaCl_2$-rich fluid inclusions with higher *T*h values (170–320 °C) in quartz associated with galena from the Jasenie-Soviansko deposit. The abundance of galena, sphalerite, and barite in these mineralizations is a consequence of the high solubility of lead and zinc as chloride complexes and barite in Cl^--rich hydrothermal solutions (Holland & Malinin 1979; Seward 1984; Ruaya & Seward 1986). There are no constraints on the temperature and pressure of formation of the chalcopyrite-tetrahedrite and galena-sphalerite assemblages from the Mlynná dolina valley other than those from the fluid inclusion study. Isochores of the inclusions of the two associations (Fig. 8b) show that estimated formation temperature of <200 °C corresponds to a pressure of 150 MPa. Chovan et al. (1995) have assumed epithermal formation conditions for the late stages of mineralization in the Dúbrava deposit. This assumption applies likely also to the Mlynná dolina valley, implying pressures significantly lower than the maximum estimate.

Conclusions

Several spatially and probably temporally separated mineral assemblages have been distinguished in the Mlynná dolina valley. Each assemblage can be assigned to one of the mineralizations distinguished by Chovan et al. (1996) in the Nízke Tatry Mts. The early arsenopyrite-pyrite assemblage corresponds to the As-Fe-Au mineralization sensu Chovan et al. (1996). The association can be linked to H_2O-CO_2-NaCl±KCl fluids with formation conditions of 280–365 °C and 150–350 MPa. The fluid inclusion-derived temperature estimates coincide with those obtained from the arsenopyrite thermometry, ranging between 320 and 380 °C. The stibnite assemblage corresponds to Fe, Cu, Pb, Sb, Bi, Ag sulphides, occurring throughout the Nízke Tatry Mts (sensu Chovan et al. 1996). The Sb sulphides from the Mlynná dolina valley have crystallized from a CO_2-unsaturated H_2O-NaCl fluid derived from

the earlier H_2O-NaCl-CO_2 fluid at temperature of 200–250 °C and pressure <100 MPa. The late chalcopyrite-tetrahedrite and galena-sphalerite assemblages coincide with the siderite veins containing Cu sulphides and Pb (galena) — base-metals mineralizations (sensu Chovan et al. 1996). The chalcopyrite-tetrahedrite assemblage can be correlated with H_2O-NaCl fluids, and the galena-sphalerite assemblage to H_2O-NaCl-$CaCl_2$ fluids, which circulated at temperatures <200 °C.

Acknowledgments: We are thankful to F. Molnár (ELTE Budapest) for his help and discussions about the issues of fluid inclusion study. We also appreciate the critical comments of N. Tabor and B. Joy. Thorough review by M.C. Boiron, R.E. Clayton, and I. Rojkovič significantly improved the quality of the manuscript. The microprobe analyses were performed by D. Ozdín (Geological Survey of Slovak Republic, Bratislava). All the thin and polished sections, as well as double-sided polished wafers were produced by cheerful V. Szabadová (Comenius University, Bratislava). The research was financially supported by a Grants VEGA No. 1/5218/98 and 1/8318/01.

References

Adamia Sh. (Ed.) 1989: Geological study of scheelite mineralization of Jasenie deposit. *Manuscript, Geofond*, Bratislava (in Russian).

Andrusov D., Koutek J. & Zoubek V. (Eds.) 1951: The results of basic, montane and geological research in the southern and northwestern part of Nízke Tatry Mts. crystalline core in 1950. *Manuscript,* Praha–Bratislava (in Czech).

Biely A. & Bezák V. 1997: Explanations to the geological map of the Nízke Tatry Mts, 1:50,000. *Geological Survey of Slovak Republic*, Bratislava, 1–232 (in Slovak).

Bodnar R.J. 1993: Revised equation and table for determining the freezing point depression of H_2O-NaCl solutions. *Geochim. Cosmochim. Acta* 57, 683–684.

Boiron M.-C., Cathelineau M., Dubessy J. & Bastoul A.M. 1990: Fluids in Hercynian Au veins from the French Variscan belt. *Mineral. Mag.* 54, 231–243.

Boiron M.-C., Cathelineau M. & Trescases J.-J. 1989: Conditions of gold-bearing arsenopyrite crystallization in the Villeranges basin, Marche-Combrailles shear zone, France: A mineralogical and fluid inclusion study. *Econ. Geol.* 84, 1340–1362.

Bowers T.S. & Helgeson H.C. 1983: Calculation of thermodynamic and geochemical consequences of nonideal mixing in the system H_2O-CO_2-NaCl on phase relations in geologic systems: Equation of state for H_2O-CO_2-NaCl fluids at high pressures and temperatures. *Geochim. Cosmochim. Acta* 47, 1247–1275.

Brown P.E. 1989: FLINCOR; a microcomputer program for the reduction and investigation of fluid-inclusion data. *Am. Mineral.* 74, 1390–1393.

Chovan M., Hurai V., Sachan H.K. & Kantor J. 1995: Origin of the fluids associated with granodiorite-hosted, Sb-As-Au-W mineralisation at Dúbrava (Nízke Tatry Mts, Western Carpathians). *Mineral. Depos.* 30, 48–54.

Chovan M., Lueders V. & Hurai V. 1999: Fluid inclusions and C,O-isotope constraints on the origin of granodiorite-hosted Sb-As-Au-W deposit at Dúbrava (Nízke Tatry Mts, Western Carpathians). *Terra Nostra 99/6. ECROFI XV Abstracts*, 71–72.

Chovan M., Slavkay M. & Michálek J. 1996: Ore mineralizations of the Ďumbierske Tatry Mts. (Western Carpathians, Slovakia). *Geol. Carpathica* 47, 6, 397–406.

Clayton R.E. & Spiro B. 2000: Sulphur, carbon and oxygen isotope studies of early Variscan mineralisation and Pb-Sb vein deposits in the Cornubian orefield: Implications for the scale of fluid movements during Variscan deformation. *Mineral. Depos.* 35, 315–331.

Collins P.L.F. 1979: Gas hydrates in CO_2-bearing fluid inclusions and the use of freezing data for estimation of salinity. *Econ. Geol.* 74, 1435–1444.

Darling R.S. 1991: An extended equation to calculate NaCl contents from final clathrate melting temperature in H_2O-CO_2-NaCl fluid inclusions: Implications for *P-T* isochore location. *Geochim. Cosmochim. Acta* 55, 3869–3871.

Davis D.W., Lowenstein T.K. & Spencer R.J. 1990: Melting behavior of fluid inclusions in laboratory-grown halite crystals in the systems NaCl-H_2O, NaCl-KCl-H_2O, NaCl-$MgCl_2$-H_2O, and NaCl-$CaCl_2$-H_2O. *Geochim. Cosmochim. Acta* 54, 591–601.

Diamond L.W. 1992: Stability of CO_2 clathrate hydrate + CO_2 liquid + CO_2 vapour + aqueous KCl-NaCl solutions: Experimental determination and application to salinity estimates of fluid inclusions. *Geochim. Cosmochim. Acta* 56, 273–280.

Groves D. I., Goldfarb R. J., Gebre-Mariam M., Hagemann S. G. & Robert F. 1998: Orogenic gold deposits: A proposed classification in the context of their crustal distribution and relationship to other gold deposit types. *Ore Geol. Rev.* 13, 7–27.

Holland H.D. & Malinin S.D. 1979: The solubility and occurrence of non-ore minerals. In: Barnes H.L. (Ed.): Geochemistry of hydrothermal ore deposits. 2nd edition. *John Wiley*, 461–508.

Krupp R.E. 1988: Solubility of stibnite in hydrogen sulfide solutions, speciation and equilibrium constants, from 25 to 350 °C. *Geochim. Cosmochim. Acta* 52, 3005–3015.

Kretschmar U. & Scott S.D. 1976: Phase relations involving arsenopyrite in the system Fe-As-S and their application. *Can. Mineral.* 14, 364–386.

Krist E., Krištín J. & Miko O. 1988: The metamorphic development of the Nízke Tatry Mts. crystalline basement (Western Carpathians). *Acta Geol. Geogr. Univ. Comen., Geol.* 44, 137–162.

Lattanzi P.F., Curti E. & Bastogi M. 1989: Fluid inclusion studies on the gold deposits in the Upper Anzasca valley, northwestern Alps, Italy. *Econ. Geol.* 84, 1382–1397.

Luptáková J., Chovan M. & Huraiová M. 2000: Pb, Zn, Cu, Sb hydrothermal mineralization at the locality Jasenie-Soviansko (Nízke Tatry Mts). In: Uher P., Broska I., Jeleň S. & Janák M. (Eds.): Mineralogical-petrological symposium Magurka 2000. 24.

Majzlan J. & Chovan M. 1997: Hydrothermal mineralization in the Mlynná dolina valley, Nízke Tatry Mts. *Miner. Slovaca* 29, 149–158 (in Slovak).

Oakes C.S., Bodnar R.J. & Simonson J.M. 1990: The system NaCl-$CaCl_2$-H_2O: I. The ice liquidus at 1 atm total pressure. *Geochim. Cosmochim. Acta* 54, 603–610.

Ortega L., Oyarzun R. & Gallego M. 1996: The Mari Rosa late Hercynian Sb-Au deposit, western Spain. *Mineral. Depos.* 31, 172–187.

Ozdín D. & Chovan M. 1999: New mineralogical and paragenetic knowledge about siderite veins in the vicinity of Vyšná Boca, Nízke Tatry Mts. *Slovak Geol. Mag.* 5, 255–271.

Ozdín D. & Pršek J. 2000: Siderite mineralization in the Nízke Tatry Mts., Western Carpathians, Slovakia. *Acta Mineralogica-Petrographica*, Supplementum 2000, 82.

Plašienka D., Grecula P., Putiš M., Kováč M. & Hovorka D. 1997: Evolution and structure of the Western Carpathians: an overview. In: Grecula P., Hovorka D. & Putiš M. (Eds.): Geological evolution of the Western Carpathians. *Miner. Slovaca — Monograph*, 1–24.

Putiš M. 1992: Variscan and Alpidic nappe structures of the Western Carpathian crystalline basement. *Geol. Carpathica* 43,

369–380.

Roedder E. 1984: Fluid inclusions. *Rev. Mineral.* 12, 1–646.

Ruaya J.R. & Seward T.M. 1986: The stability of chlorozinc(II) complexes in hydrothermal solutions up to 350 °C. *Geochim. Cosmochim. Acta* 50, 5, 651–661.

Sachan H.K. & Chovan M. 1991: Thermometry on arsenopyrite-pyrite mineralisation in the Dúbrava antimony deposit (Western Carpathians). *Geol. Carpathica* 42, 265–269.

Seward T.M. 1973: Thio complexes of gold and the transport of gold in hydrothermal ore solutions. *Geochim. Cosmochim. Acta* 37, 379–399.

Seward T.M. 1984: The formation of lead(II) chloride complexes to 300 °C: A spectrophotometric study. *Geochim. Cosmochim. Acta* 48, 1, 121–134.

Sharp Z.D., Essene E.J. & Kelly W.C. 1985: A re-examination of the arsenopyrite geothermometer: Pressure consideration and application to natural assemblages. *Can. Mineral.* 23, 517–534.

Slavkay M. & Chovan M. 1996: A review of metallic ore mineralizations of the Nízke Tatry Mts. In: Grecula P. (Ed.): Variscan metallogeny of the Alpine orogenic belt. *Miner. Slovaca — Monography*, 239–250.

Smirnov A. 2000: Sb-Au mineralization in the vicinity of Nižná Boca (Nízke Tatry Mts). *Unpublished thesis,* Comenius University, Bratislava, 1–131.

Stankovič J. 1976: Raw materials in the map portion Mýto pod Ďumbierom 1:25,000. *Dionýz Štúr Geological Institute*, Bratislava (in Slovak).

Turan J. 1961: About the ore mineralization at Trangoška and some occurrences in the Bystrá and Mlyná valleys on the southern slopes of the Nízke Tatry Mts. *Geol. Práce, Zpr.* 23, 85–114 (in Slovak).

Vaughan D.J. & Craig J.R. 1997: Sulfide ore mineral stabilities, morphologies, and intergrowth textures. In: Barnes H.L. (Ed.): Geochemistry of Hydrothermal Ore Deposits. 2nd edition. *John Wiley,* 1–424.

Williams-Jones A.E. & Normand C. 1997: Controls of mineral parageneses in the system Fe-Sb-S-O. *Econ. Geol.* 92, 308–324.

Zhang Y.-G. & Frantz J.D. 1987: Determination of the homogenization temperatures and densities of supercritical fluids in the system NaCl-KCl-$CaCl_2$-H_2O using synthetic fluid inclusions. *Chem. Geol.* 64, 335–350.